

Mechanical quantum resonators

A. N. Cleland* and M. R. Geller†

*Department of Physics, University of California, Santa Barbara CA 93106 USA

†Department of Physics and Astronomy, University of Georgia, Athens, Georgia 30602 USA

Abstract. We describe the design for a solid-state quantum computational architecture based on the integration of GHz-frequency mechanical resonators with Josephson phase qubits, which have the potential for demonstrating a variety of single- and multi-qubit operations critical to quantum computation. The computational qubits are eigenstates of large-area, current-biased Josephson junctions. Two or more qubits are capacitively coupled to a piezoelectric nanoelectromechanical disk resonator, which enables coherent coupling of the qubits. The integrated system is analogous to one or more few-level atoms (the Josephson junction qubits) in an electromagnetic cavity (the nanomechanical resonator). However, here we can individually tune the level spacing of the “atoms” and control their “electromagnetic” interaction strength. We show that quantum states prepared in a Josephson junction can be passed to the nanomechanical resonator and stored there, and then can be passed back to the original junction or transferred to another with high fidelity. The resonator can also be used to produce maximally entangled Bell states between a pair of Josephson junctions.

Keywords: Josephson junction; qubit; quantum computation

PACS: 03.67.Lx, 85.25.Cp, 85.85.+j

The lack of easily fabricated physical qubit elements, having both sufficiently long quantum-coherence lifetimes and the means for producing and controlling their entanglement, remains the principal roadblock to building a large-scale quantum computer. Superconducting devices have been understood for several years to be natural candidates for quantum computation, given that they exhibit robust macroscopic quantum behavior [1]. Demonstrations of long-lived Rabi oscillations in current-biased Josephson tunnel junctions [2, 3], and of both Rabi oscillations and Ramsey fringes in a Cooper-pair box [5], have generated significant new interest in the potential for superconductor-based quantum computation [6]. Coherence times τ_ϕ up to $5\mu\text{s}$ have been reported in the current-biased devices [2], with corresponding quantum-coherent quality factors $Q_\phi \equiv \tau_\phi \Delta E / \hbar$ of the order of 10^5 , indicating that these systems should be able to perform many logical operations during the available coherence lifetime (here ΔE is the qubit energy-level separation).

Here we describe a proposal that GHz-frequency nanoelectromechanical resonators can be used to coherently couple two or more current-biased Josephson junction devices together to make a flexible and scalable solid-state quantum-information-processing architecture [7]. The computational qubits are the energy eigenstates of the junctions. These superconducting phase qubits are capacitively coupled to a piezoelectric dilational disk resonator, cooled on a dilution refrigerator to the quantum limit. We show that the integrated system is analogous to one or more few-level atoms in an electromagnetic cavity (the resonator). We can tune *in situ* the energy level spacing of each “atom”, and control the “electromagnetic” interaction strength. This analogy makes it clear that our design is sufficiently flexible to be able to carry out any operation that can be done

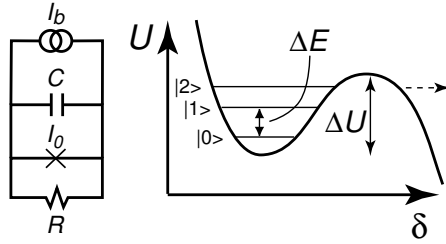


FIGURE 1. *Left:* Equivalent-circuit model for a current-biased Josephson junction. A capacitance C and resistance R in parallel with an ideal Josephson element with critical current I_0 , all sharing a bias current I_b . *Right:* Potential in the cubic $s \rightarrow 1^-$ limit.

using other architectures, provided that there is enough coherence.

Several investigators have proposed the use of LC resonators [8], superconducting cavities [9], or other types of oscillators, to couple junctions together. Resonator-based coupling schemes, such as the one proposed here, have additional functionality resulting from the ability to tune the qubits relative to the resonator frequency, as well as to each other. By tuning the junctions in and out of resonance with the nanomechanical resonator, qubit states prepared in a junction can be passed to the resonator and stored there, and can later be passed back to the original junction or transferred to another junction with high fidelity. The resonator can also be used to produce controlled entangled states between a pair of junctions. The use of mechanical resonators to mediate multi-qubit operations in junction-based quantum information processors has not (to the best of our knowledge) been considered previously, but our proposal builds on the interesting recent work by Armour *et al.* [10] and Irish *et al.* [11].

Our implementation uses large-area current-biased Josephson junctions, with capacitance C and critical current I_0 , as shown in Fig. 1. The largest relevant energy scale is the Josephson energy $E_J \equiv \hbar I_0 / 2e$, with charging energy $E_c \equiv (2e)^2 / 2C \ll E_J$. The dynamics of the phase difference δ is that of a particle of mass $M = \hbar^2 C / 4e^2$ moving in an effective potential $U(\delta) \equiv -E_J(\cos \delta + s \delta)$, where $s \equiv I_b / I_0$ is the dimensionless bias current [12]. When $0 < s < 1$, $U(\delta)$ has metastable minima, separated from the continuum by a barrier of height ΔU , also shown in Fig. 1. The small-oscillation plasma frequency is $\omega_p = \omega_{p0} (1 - s^2)^{1/4}$, with $\omega_{p0} = \sqrt{2E_J E_c} / \hbar$. The Hamiltonian for an isolated junction is $H_J = -E_c d^2 / d\delta^2 + U(\delta)$, with quasi-bound states in the minima with energies ε_m . The lowest energy quasi-bound states $|0\rangle$ and $|1\rangle$ define the phase qubit, with $\Delta E \equiv \varepsilon_1 - \varepsilon_0$ the level spacing. We focus here on a single resonator coupled to one and two junctions; extensions to larger systems will be addressed in future work. The basic two-junction circuit is shown in Fig. 2. The disk-shaped element is the nanomechanical resonator, consisting of a piezoelectric crystal sandwiched between split metal electrodes, and the junctions are the crossed boxes.

The nanomechanical resonator is designed to have a fundamental thickness-resonance frequency $\omega_0 / 2\pi$ of a few GHz, and a high quality factor Q . Piezoelectric dilatational resonators with frequencies in this range, and with room-temperature quality factors around 10^3 , have been fabricated from sputtered AlN [13]. We have performed RF network measurements down to 4.2 K for a similar piezoelectric 1.8 GHz resonator. The

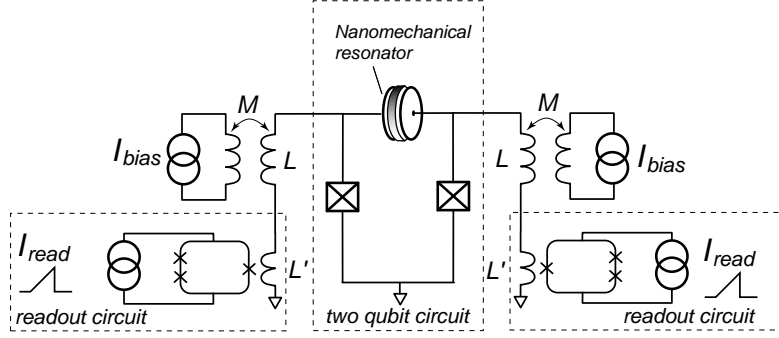


FIGURE 2. Two phase qubits coupled to a piezoelectric resonator.

observed low-temperature Q of 3500 corresponds to an energy lifetime τ of more than 300ns, sufficient for the operations described below. Upon cooling to 20mK, the 1.8 GHz dilatational mode will be in the quantum regime, with a probability of thermally occupying the first excited (one-phonon) state of about 10^{-2} . Using dilatational-phonon creation and annihilation operators, the resonator Hamiltonian is $H_{\text{res}} = \hbar\omega_0 a^\dagger a$.

An elastic strain in the resonator produces, through the piezoelectric effect, a charge q on the capacitor enclosing it, corresponding to a current \dot{q} . A model for a disk resonator of radius R and thickness b leads to $q = C_{\text{res}}(V - e_{33}bU_{zz}/\epsilon_{33})$, where $C_{\text{res}} = \epsilon_{33}\pi R^2/b$ is the resonator capacitance, V the voltage across it, e_{33} and ϵ_{33} the relevant elements of the piezoelectric modulus and dielectric tensors, and U_{zz} the spatially averaged strain. Strain induces an electric field $E_z = e_{33}U_{zz}/\epsilon_{33}$ in the piezoelectric, and a charge of magnitude $\tilde{C}_{\text{res}}E_z b$ on the electrodes, where \tilde{C}_{res} is a piezoelectrically-enhanced capacitance. The resonator adds the capacitance \tilde{C}_{res} in parallel with the junction capacitance, reducing the charging energy E_c to $2e^2/(C + \tilde{C}_{\text{res}})$.

Quantizing the vibrational modes of the resonator in the presence of the appropriate mechanical and electrodynamic boundary conditions leads to a Hamiltonian for a single junction coupled to a resonator $H = H_J + H_{\text{res}} + \delta H$, where $\delta H = -ig(a - a^\dagger)\delta$, and g is a real-valued coupling constant with dimensions of energy. The eigenstates of $H_J + H_{\text{res}}$ are $|mn\rangle \equiv |m\rangle_J \otimes |n\rangle_{\text{res}}$, with energies $E_{mn} = \epsilon_m + \hbar\omega_0 n$ (n is the resonator phonon occupation number), and an arbitrary state can be expanded as $|\psi(t)\rangle = \sum_{mn} c_{mn}(t) e^{-iE_{mn}t/\hbar} |mn\rangle$.

We first show that we can pass a qubit state from a junction to the resonator and store it there, using the adiabatic approximation combined with the rotating-wave approximation (RWA) [16]. We assume that s changes slowly on the time scale $\hbar/\Delta E$, and work at zero temperature. From the RWA, neglecting population and phase relaxation, we obtain from the equations of motion for the coefficients $c_{mn}(t)$.

At time $t = 0$ we prepare the junction in the state $\alpha|0\rangle_J + \beta|1\rangle_J$, leaving the resonator in the ground state $|0\rangle_{\text{res}}$. We then allow the junction and resonator to interact on resonance for a time interval $\Delta t = \pi/\Omega_0$, where Ω_0 is the vacuum Rabi frequency. We then bring the systems out of resonance and the resonator is found to be in the same pure state, apart from expected phase factors. The junction state has actually been swapped with that of the resonator.

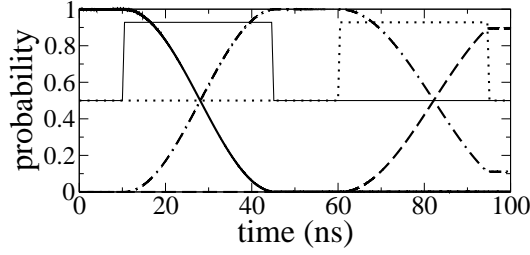


FIGURE 3. Qubit transfer between two junctions. Solid curve is $|c_{100}|^2$, dashed-dotted curve is $|c_{001}|^2$, and dashed curve is $|c_{010}|^2$. Thin solid and dotted curves show s_1 and s_2 , respectively.

We have also solved the exact equations numerically, including all quasi-bound junction states present. The initial state is $|10\rangle$, corresponding to the case $\alpha = 0$, $\beta = 1$. After 10 ns, the bias current is adiabatically changed to bring the qubit in resonance with $\hbar\omega_0$. The junction is held in resonance for half a Rabi period, and then detuned. $s(t)$ has a trapezoidal shape with a crossover time of 0.5 ns. The storage operation is successful, and the magnitudes of the final probability amplitudes, are extremely close to the desired RWA values. The phases of the c_{mn} after storage, however, are not correctly given by the RWA unless $g/\Delta E$ is much smaller.

To transfer a qubit state $\alpha|0\rangle + \beta|1\rangle$ between two junctions, the state is loaded into the first junction and the bias current s_1 adjusted to bring that junction into resonance with the resonator for half a Rabi period. This stores the junction state in the resonator. After the first junction is taken out of resonance, the second one is brought into resonance for half a Rabi period, passing the state to the second junction. We have simulated this operation, assuming two identical junctions as in Fig. 2. Our results are shown in Fig. 3, where $c_{m_1 m_2 n}$ is the probability amplitude to find the system in the state $|m_1 m_2 n\rangle$, with m_1 and m_2 labelling the states of the two junctions and n the phonon occupation number of the resonator.

Finally, we can prepare an entangled state of two junctions connected to a common resonator by bringing the first junction into resonance with the resonator for one-quarter of a Rabi period, which produces the state $(|100\rangle + |001\rangle)/\sqrt{2}$. After bringing the second junction into resonance for half a Rabi period, the state of the resonator and second junction are swapped as $|001\rangle \rightarrow -|010\rangle$, leaving the system in the state $(|100\rangle - |010\rangle)/\sqrt{2}$, where the resonator is in the ground state and the junctions are maximally entangled. Our simulations of this operation, the results of which are presented in Fig. 4, demonstrate successful entanglement with a fidelity of 95%. The system parameters are the same as in Fig. 3.

The quantum-information-processing operations described here require a minimum coherence time of order 100 ns, a time already demonstrated in the phase qubit. More extensive operations could be performed with a coherence time of a few hundred nanoseconds, which have recently been achieved in the phase qubit [20]. The mechanical resonator must also achieve similar coherence times; using standard results for the coherence time of a particle coupled to a dissipative environment [21], we estimate the quantum coherence time of an n -phonon state to be the lesser of $\tau \approx \hbar Q/k_B T(n + 1/2)$ and the energy decay lifetime Q/ω_0 . At 20 mK, the $|1\rangle$ state of our resonator is determined

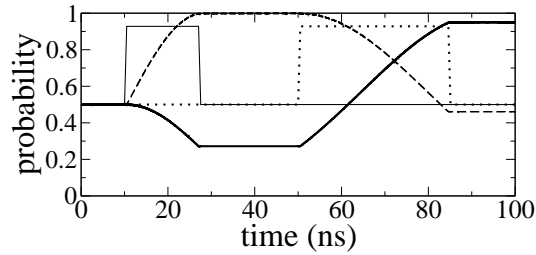


FIGURE 4. JJ entanglement. Dashed curve is the probability to be in the state (in the interaction representation) $(|100\rangle + |001\rangle)/\sqrt{2}$, and thick solid curve is for $(|100\rangle - |010\rangle)/\sqrt{2}$. Thin solid and dotted curves are s_1 and s_2 .

by the decay lifetime, which for $Q \approx 3500$ is about 300 ns.

REFERENCES

1. Y. Makhlin, G. Schön, and A. Shnirman, *Rev. Mod. Phys.* **73**, 357 (2001).
2. Y. Yu, S. Han, X. Chu, S.-I. Chu, and Z. Wang, *Science* **296**, 889 (2002).
3. J. M. Martinis, S. Nam, J. Aumentado, and C. Urbina, *Phys. Rev. Lett.* **89**, 117901 (2002).
4. A. J. Berkley et al. *Science* **300**, 1548 (2003). F. W. Strauch et al., *Phys. Rev. Lett.* **91**, 167005 (2003).
5. Y. Nakamura, Yu. A. Pashkin, and J. S. Tsai, *Nature* **398**, 786 (1999). D. Vion et al., *Science* **296**, 886 (2002). T. Yamamoto, Yu. A. Pashkin, O. Astafiev, Y. Nakamura, and J. S. Tsai, *Nature* **425**, 941 (2003).
6. A. J. Leggett, *Science* **296**, 861 (2002).
7. A. N. Cleland and M. L. Geller, *Phys. Rev. Lett.* **93**, 70501 (2004).
8. A. Shnirman, G. Schön, and Z. Hermon, *Phys. Rev. Lett.* **79**, 2371 (1997). Y. Makhlin, G. Schön, and A. Shnirman, *Nature* **398**, 305 (1999). A. Blais, A. M. van den Brink, and A. M. Zagoskin, *Phys. Rev. Lett.* **90**, 127901 (2003). F. Plastina and G. Falci, *Phys. Rev. B* **67**, 224514 (2003).
9. O. Buisson and F. W. J. Hekking, in *Macroscopic Quantum Coherence and Quantum Computing*, edited by D. V. Averin, B. Ruggiero, and P. Silvestrini (Kluwer, New York, 2001), p. 137. F. Marquardt and C. Bruder, *Phys. Rev. B* **63**, 54514 (2001).
10. A. D. Armour, M. P. Blencowe, and K. C. Schwab, *Phys. Rev. Lett.* **88**, 148301 (2002).
11. E. K. Irish and K. Schwab, *Phys. Rev. B* **68**, 155311 (2003).
12. A. Barone and G. Paterno, *Physics and Applications of the Josephson Effect* (Wiley, New York, 1982).
13. R. Ruby, P. Bradley, J. Larson, Y. Oshmyansky, and D. Figueredo, *Tech. Digest 2001 IEEE Intl. Solid-State Circuits Conf.*, p. 120 (2001).
14. X. M. H. Huang, C. A. Zorman, M. Mehregany, and M. L. Roukes, *Nature* **421**, 496 (2003).
15. A. N. Cleland, M. Pophristic and I. Ferguson, *Appl. Phys. Lett.* **79**, 2070 (2001).
16. M. O. Scully and M. S. Zubairy, *Quantum Optics* (Cambridge University Press, Cambridge, 1997).
17. X. Maître, E. Hagley, G. Nogues, C. Wunderlich, P. Goy, M. Brune, J. M. Raimond, and S. Haroche, *Phys. Rev. Lett.* **79**, 769 (1997).
18. E. Hagley, X. Maître, G. Nogues, C. Wunderlich, M. Brune, J. M. Raimond, and S. Haroche, *Phys. Rev. Lett.* **79**, 1 (1997).
19. J. M. Martinis, private communication.
20. J. M. Martinis, S. Nam, J. Aumentado, and K. M. Lang, *Phys. Rev. B* **67**, 94510 (2003).
21. E. Joos, in *Decoherence and the Appearance of a Classical World in Quantum Theory*, edited by D. Giulini et al. (Springer-Verlag, Berlin, 1996), p. 35.